

Enhanced di-Higgs Production in the Complex Higgs Singlet Model

S. Dawson^a and M. Sullivan^{a,b}

^a*Department of Physics, Brookhaven National Laboratory, Upton, N.Y., 11973, U.S.A.*

^b*Department of Physics and Astronomy, University of Kansas, Lawrence, Kansas, 66045 USA*

(Dated: March 8, 2024)

Abstract

We consider the Standard Model (SM) extended by the addition of a complex scalar singlet, with no assumptions about additional symmetries of the potential. This model provides for resonant di-Higgs production of Higgs particles with different masses. We demonstrate that regions of parameter space allowed by precision electroweak measurements, experimental limits on single Higgs production, and perturbative unitarity allow for large di-Higgs production rates relative to the SM rates. In this scenario, the dominant production mechanism of the new scalar states is di-Higgs production. Results are presented for $\sqrt{S} = 13, 27$ and 100 TeV .

I. INTRODUCTION

The exploration of the Higgs sector is a primary focus of the LHC physics program, with measurements of the Higgs couplings to fermions and gauge bosons, the Higgs mass, and Higgs CP properties becoming ever more precise. Very little is known, however, about the Higgs tri-linear and quartic self-couplings which are unambiguously predicted in the Standard Model (SM). The SM Higgs tri-linear coupling can be most sensitively probed by double Higgs production through gluon fusion which unfortunately has a very small rate[1], even at high energy and high luminosity[2]. The best current limit on double Higgs production is from the ATLAS experiment[3], $\sigma(pp \rightarrow hh)/\sigma(pp \rightarrow hh)_{SM} < 29$, with prospects for only modest improvements at higher luminosity. A definitive measurement of the SM tri-linear Higgs self-coupling appears out of reach at the LHC[4–6].

Given the small SM rate for double Higgs production, it is an excellent place to search for Beyond the SM (BSM) physics. In the presence of a scalar resonance coupling to the SM-like Higgs boson, the double Higgs rate can be significantly enhanced. This can occur in the MSSM and the NMSSM, for example. The simplest possibility is to add a hypercharge-0 real scalar to the model which interacts with SM fermions and gauge bosons only through the mixing with the Higgs doublet. The LHC phenomenology in the context of the real singlet model has been extensively studied in the literature[7–14]. When the most general scalar potential (without the imposition of a Z_2 symmetry) is considered, the real singlet model can have a first order electroweak phase transition[15–18] for some values of the parameters.

The complex scalar singlet extension has new features beyond the real singlet case. It has several phases, 2 of which can accommodate a dark matter candidate[19, 20]. In the broken phase of this model (which is the subject of this work) there are 3 neutral scalar particles which mix to form the mass eigenstates, one of which is the 125 *GeV* scalar. Final states with 2 different mass scalar particles can be resonantly produced in this scenario and there are large regions of parameter space where the couplings of the new scalars to SM particles are highly suppressed, making the dominant production mechanism of the new scalars the Higgs decays to other Higgs-like particles. The resonant production of two different mass Higgs particles is a smoking gun for this class of theories.

We study the most general case of a complex scalar singlet extension of the SM, without the introduction of any new symmetries for the potential. The complex singlet model has

been previously studied imposing a softly broken $U(1)$ symmetry and benchmark points described for the study of the decay of the heavy scalar to the SM Higgs boson and the lighter scalar of the model[21, 22]. The parameter space of the model we study is larger, allowing for new phenomenology. The basic features of the model are discussed in Section II and the limits on the model from perturbativity, unitarity and the oblique parameters are presented in Sec. III. Our most interesting results are the implications for double Higgs studies and the description of scenarios where one of the new Higgs bosons is predominantly produced in association with the 125 GeV boson. This is discussed in Sec. IV.

II. MODEL

We consider a model containing the SM $SU(2)$ doublet, Φ , and a complex scalar singlet, S_c . Since S_c has hypercharge -0 it does not couple directly to SM fermion or gauge fields, and its tree level interactions with SM fermions and gauge bosons result entirely from mixing with Φ . The most general renormalizable scalar potential is[23],

$$\begin{aligned} \mathcal{V}(\Phi, S_c) = & \frac{\mu^2}{2}\Phi^\dagger\Phi + \frac{\lambda}{4}(\Phi^\dagger\Phi)^2 + \left(\frac{1}{4}\delta_1\Phi^\dagger\Phi S_c + \frac{1}{4}\delta_3\Phi^\dagger\Phi S_c^2 + a_1 S_c \right. \\ & + \frac{1}{4}b_1 S_c^2 + \frac{1}{6}e_1 S_c^3 + \frac{1}{6}e_2 S_c |S_c|^2 + \frac{1}{8}d_1 S_c^4 + \frac{1}{8}d_3 S_c^2 |S_c|^2 + h.c. \Big) \\ & + \frac{1}{4}d_2(|S_c|^2)^2 + \frac{\delta_2}{2}\Phi^\dagger\Phi |S_c|^2 + \frac{1}{2}b_2 |S_c|^2, \end{aligned} \quad (1)$$

where $a_1, b_1, e_1, e_2, d_1, d_3, \delta_1$ and δ_3 are complex. After spontaneous symmetry breaking, in unitary gauge,

$$\Phi = \begin{pmatrix} 0 \\ \frac{h+v}{\sqrt{2}} \end{pmatrix}, \quad S_c = \frac{1}{\sqrt{2}} \left(S + v_S + i(A + v_A) \right). \quad (2)$$

Since we have included all allowed terms in Eq. 1, the coefficients can always be redefined such that $v_S = v_A = 0$. This makes the potential of Eq. 1 identical to that obtained by adding 2 real singlets to the SM and there is no CP violation. Previous work[21, 23] imposed a global $U(1)$ symmetry or a Z_2 symmetry to eliminate some of the terms in the potential, making the shift to $v_S = v_A = 0$ in general not possible.

The mass eigenstate fields are h_1, h_2, h_3 (masses m_1, m_2, m_3) are found from the rotation,

$$\begin{pmatrix} h_1 \\ h_2 \\ h_3 \end{pmatrix} = V \begin{pmatrix} h \\ S \\ A \end{pmatrix}, \quad (3)$$

where V is a 3×3 unitary matrix with,

$$V \equiv \begin{pmatrix} c_1 & -s_1 c_3 & -s_1 s_3 \\ s_1 c_2 & c_1 c_2 c_3 - s_2 s_3 & c_1 c_2 s_3 + s_2 c_3 \\ s_1 s_2 & c_1 s_2 c_3 + c_2 s_3 & c_1 s_2 s_3 - c_2 c_3 \end{pmatrix} \quad (4)$$

and we abbreviate $c_i = \cos \theta_i$, etc. Note that the phase usually associated with the CKM-like mixing matrix does not appear since the mass matrix in terms of the real fields h , S , and A is strictly real by hermiticity. Since all allowed terms are included in Eq. 1, we are free to perform a field redefinition $S_c \rightarrow S_c e^{i\phi}$ while leaving the form of the potential unchanged. We choose to take $S_c \rightarrow S_c e^{i\theta_3}$. This results in the field redefinitions,

$$\begin{pmatrix} h \\ S \\ A \end{pmatrix} \rightarrow \begin{pmatrix} 1 & 0 & 0 \\ 0 & c_3 & -s_3 \\ 0 & s_3 & c_3 \end{pmatrix} \begin{pmatrix} h \\ S \\ A \end{pmatrix}, \quad (5)$$

which, when combined with Eqs. 3 and 4 with matrix multiplication, leads to a simplified mixing matrix,

$$V \rightarrow \begin{pmatrix} c_1 & -s_1 & 0 \\ s_1 c_2 & c_1 c_2 & s_2 \\ s_1 s_2 & c_1 s_2 & -c_2 \end{pmatrix}. \quad (6)$$

So we see that performing a suitable phase rotation is equivalent to setting $\theta_3 = 0$. For the rest of the paper, we use this convention to eliminate θ_3 .

We take as inputs to our scans,

$$v = 246 \text{ GeV}, m_1 = 125 \text{ GeV}, m_2, m_3, \theta_1, \theta_2, \delta_2, \delta_3, d_1, d_2, d_3, e_1, e_2 \quad (7)$$

where δ_3, d_1, d_3, e_1 and e_2 can be complex and are defined in Eq. 1.

The SM-like Higgs boson is identified with h_1 with $m_1 = 125 \text{ GeV}$. The couplings of h_1 to SM particles are suppressed by a factor c_1 relative to the SM rate. The states are ordered according to their couplings to SM particles. h_1 has the strongest couplings to SM particles,

h_2 couplings are suppressed by $s_1 c_2$ relative to the SM couplings, and h_3 couplings are the smallest, and are suppressed by $s_1 s_2$ relative to SM couplings. The mass ordering of h_2 and h_3 is arbitrary. The ATLAS experiment restricts the value of c_1 to be,

$$c_1 = |V_{11}| > 0.94, \quad (8)$$

at 95% confidence level using Run-1 Higgs coupling fits[24]. Similarly, a global fit to Higgs coupling strengths by CMS and ATLAS[25],

$$\mu = 1.09 \pm .11, \quad (9)$$

yields an identical limit on c_1 .

III. LIMITS FROM PERTURBATIVITY, OBLIQUE PARAMETERS AND UNITARITY

The parameters of the model must satisfy constraints from electroweak precision measurements, searches for heavy Higgs bosons, and limits from perturbative unitarity, along with the restrictions from single Higgs production discussed in the previous section. Fits to the oblique parameters place strong limits on the allowed scalar masses and mixings. Analytic results for a model with 2 additional scalar singlets are given in Ref. [26]. For $m_i \gg M_W, M_Z$, the approximate contributions are ,

$$\begin{aligned} \Delta\mathcal{S} &\sim (1 - |V_{11}|^2) \mathcal{S}_{SM} + \frac{1}{12\pi} \sum_{i=1,2,3} |V_{i1}|^2 \log\left(\frac{m_i^2}{m_1^2}\right) \\ \Delta\mathcal{T} &\sim (1 - |V_{11}|^2) \mathcal{T}_{SM} - \frac{3}{16\pi c_W^2} \sum_{i=1,2,3} |V_{i1}|^2 \log\left(\frac{m_i^2}{m_1^2}\right) \\ \Delta\mathcal{U} &\sim (1 - |V_{11}|^2) \mathcal{U}_{SM}. \end{aligned} \quad (10)$$

The restrictions from the oblique parameters[27] on $V_{21} = s_1 c_2$ for the minimum value of $c_1 = .94$ allowed by single Higgs production are shown on the LHS and for $c_1 = .96$ on the RHS of Fig. 1. TeV scale masses require quite small values of V_{21} , which is the parameter that determines the coupling of h_2 to SM particles. The flat portions of the curves for small m_2 in Fig. 1 represent the imposed limit on θ_1 from single Higgs production. As this limit becomes stronger, the limits from oblique parameters becomes less and less relevant. As the h_1 couplings become more and more SM-like ($\theta_1 \rightarrow 0$), the allowed coupling of h_2 to SM

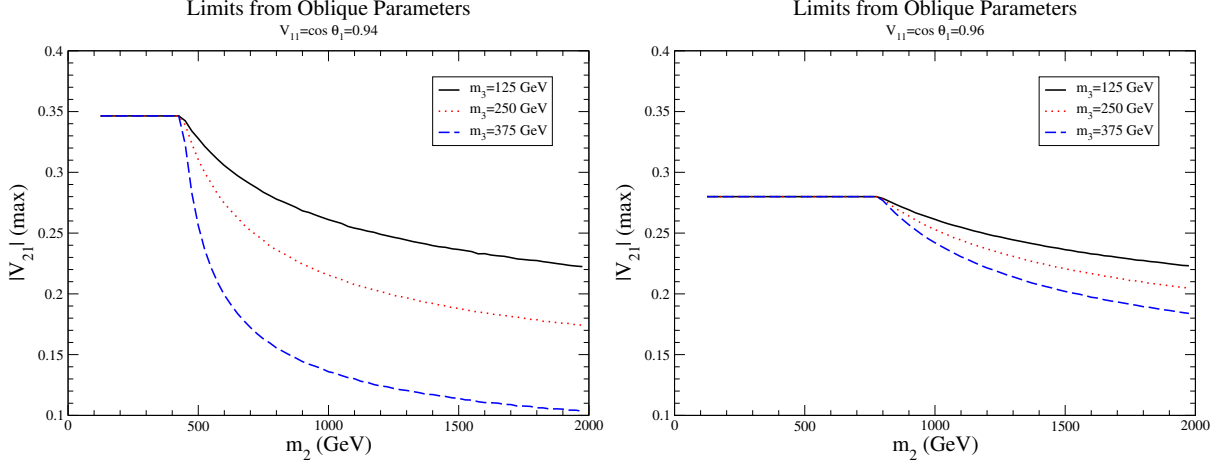


FIG. 1: Limits on m_2 for allowed couplings of h_1 to SM particles [$\cos \theta_1 = .94$ (LHS) and $\cos \theta_1 = .96$ (RHS)] for various values of m_3 using the oblique parameter ($\mathcal{S}, \mathcal{T}, \mathcal{U}$) limits of Ref. [27].

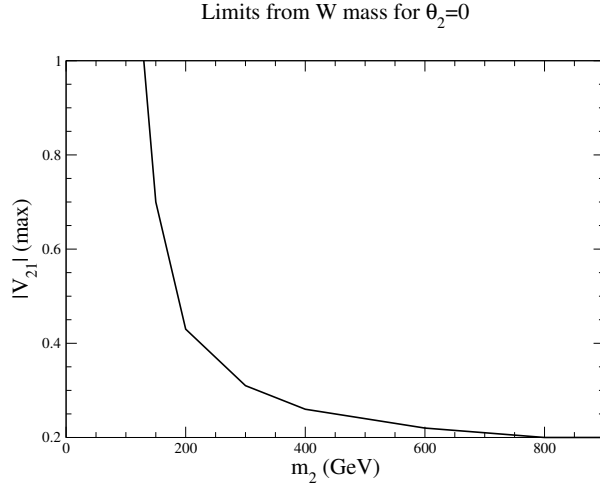


FIG. 2: Maximum allowed value of V_{21} from the W mass measurement as a function of m_2 in the real singlet model and in the complex singlet model with $\theta_2 = 0$ from Ref. [30].

particles becomes highly suppressed. The constraints from the oblique parameters shown in Fig. 1 are consistent with those obtained in the real singlet model in Ref. [10]. For the values of θ_2 allowed by Fig. 1, the direct searches, $pp \rightarrow h_2(h_3) \rightarrow W^+W^-$ do not provide additional restrictions on V_{21} [28, 29].

In the real singlet model, much stronger constraints are placed on the parameters from the W boson mass than from the oblique parameters [30, 31]. For example, in the real singlet model for $m_2 = 1 \text{ TeV}$, the W mass measurement requires $|V_{21}| < .19$. For $\theta_2 = 0$, h_3 does

not couple to SM particles and the results of Refs. [30, 31] can be applied directly to the complex singlet case. The results of Ref. [30] are shown in Fig. 2. The calculation of the limit from the W mass in the complex singlet model for non-zero θ_2 is beyond the scope of this paper and involves contributions from all 3 Higgs bosons and could potentially yield interesting limits. The limits from the oblique parameters in the complex singlet case, (Fig. 1), demonstrates that the dependence of the limits on m_3 is non-trivial.

The quartic couplings in the potential are strongly limited by the requirement of perturbative unitarity of the $2 \rightarrow 2$ scattering processes[32]. We compute the $J = 0$ partial waves, a_0 , in the high energy limit where only the quartic couplings contribute and require $|a_0| < \frac{1}{2}$. The contributions from the tri-linear couplings are suppressed at high energy and do not contribute in this limit. For example, we find the restriction from the process, $(SS)/\sqrt{2} \rightarrow (SS)/\sqrt{2}$,

$$Re(d_1 + d_2 + d_3) \lesssim \frac{32\pi}{3}. \quad (11)$$

Similarly, from $hS \rightarrow hS$, we find,

$$Re(\delta_2 + \delta_3) \lesssim 16\pi. \quad (12)$$

Looking at the eigenvectors for neutral CP even scattering processes,

$$\left\{ \omega^+ \omega^-, \frac{zz}{\sqrt{2}}, \frac{hh}{\sqrt{2}}, hS, hA, \frac{SS}{\sqrt{2}}, \frac{AA}{\sqrt{2}}, AS \right\}, \quad (13)$$

(ω^\pm, z are the Goldstone bosons), we find the generic upper limits on the real and imaginary quartic couplings,

$$Re(d_i), Im(d_i) \lesssim \frac{32\pi}{3}, i = 1, 2, 3$$

$$\delta_2, Re(\delta_3), Im(\delta_3) \lesssim 16\pi. \quad (14)$$

These upper limits are conservative bounds, and more stringent bounds are obtained from looking at the eigenvalues of the 8 by 8 scattering matrix. These upper bounds on the parameters involve finding solutions to higher order polynomials and do not have simple analytic solutions. Thus, the bounds from perturbative unitarity are determined numerically and imposed in the scans of the next section.

The tri-linear Higgs couplings depend on the scalar masses and could potentially become large. In the limit of small mixing, $\theta_1 \ll 1$ and $\theta_2 = 0$, the $h_2 h_1 h_1$ coupling is,

$$\lambda_{211} \rightarrow \sin \theta_1 \left\{ \frac{2m_1^2}{v} \left(1 + \frac{m_2^2}{2m_1^2} \right) - v \left(\delta_2 + Re(\delta_3) \right) \right\}, \text{ small angle limit} \quad (15)$$

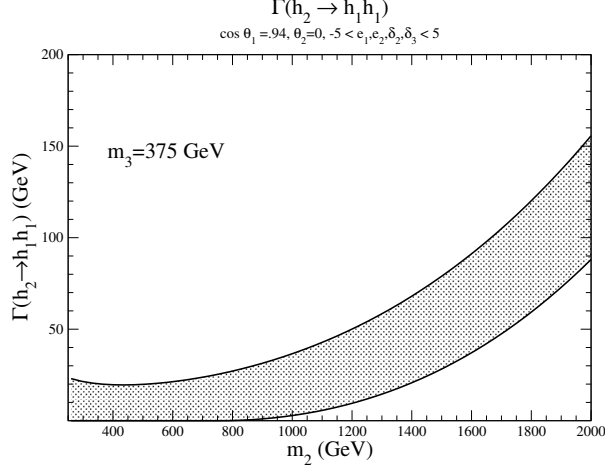


FIG. 3: Decay width for $h_2 \rightarrow h_1 h_1$ when all parameters are taken real and δ_2 and δ_3 are scanned over.

and we see that the growth of λ_{211} with large m_2 is mitigated by the $\sin(\theta_1)$ suppression. The decay width for $h_2 \rightarrow h_1 h_1$ is[11],

$$\Gamma(h_2 \rightarrow h_1 h_1) = \frac{\lambda_{211}^2}{32\pi m_2} \sqrt{1 - \frac{4m_1^2}{m_2^2}}. \quad (16)$$

In Fig. 3, we have taken all parameters real and scanned over $-5 < \delta_2, \delta_3 < 5$ for fixed m_3 , θ_1 and θ_2 . The dependence on e_1 and e_2 is minimal in the small angle limit, as demonstrated in Eq. 15. In all cases, we have $\Gamma(h_2 \rightarrow h_1 h_1) \ll m_2$, showing that there is no problem with the tri-linear couplings becoming non-perturbative in the small angle limit. Increasing the range we scan over changes the numerical results, but $\Gamma(h_2 \rightarrow h_1 h_1)/m_2$ is always $\ll 1$.

Finally, we require that the parameters correspond to an absolute minimum of the potential. This has been extensively studied for the real singlet model in Refs. [13, 15, 19] and analytic results derived. For the case of the complex singlet, we scan over parameter space for numerically allowed values of the parameters[20] and do not obtain an analytic solution.

IV. RESULTS

In the limit of $\theta_2 \rightarrow 0$, (as suggested by the single Higgs rates), the scalar h_3 does not couple directly to SM particles and it can only be observed through di-Higgs production. We will consider h_3 to be in the $100 - 400 \text{ GeV}$ mass range. The largest production rate at the LHC is through the resonant process $gg \rightarrow h_2 \rightarrow h_1 h_3$. The complex singlet model is thus

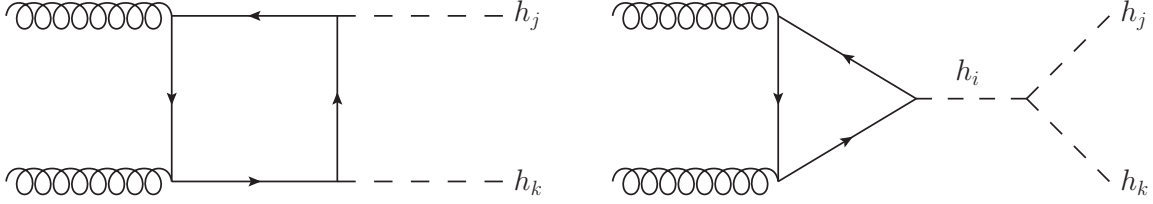


FIG. 4: Feynman diagrams for the production of $h_j h_k$, $i, j, k = 1, 2, 3$.

an example of new physics that will first be seen in the study of di-Higgs resonances[22, 33]. We perform a scan over the parameters of Eq. 7, subject to the restrictions discussed in the previous section¹. We always fix $c_1 = 0.94$ and consider the 2 cases, $\theta_2 = 0$ and $\theta_2 = \frac{\pi}{12}$.

For the allowed parameter space, we compute the amplitude for $gg \rightarrow h_1 h_3$ shown in Fig. 4. Analytic results in the context of the MSSM are given in Ref. [1]. We use the central NLO LHAPDF set[34, 35], with $\mu_R = \mu_F = M_{hh}$ ². In Fig. 5, we show the invariant M_{hh} spectrum for resonant $h_1 h_3$ production compared to the SM $h_1 h_1$ spectrum at 13 TeV. The complex singlet model curves are more sharply peaked than those of the SM and demonstrate a significant enhancement of the rate relative to the SM double Higgs rate for the parameters we have chosen. The spectrum has only a small dependence on θ_2 , visible at high M_{hh} . We have included a finite width for m_2 in the calculation: For $m_2 = 400$ GeV and $m_3 = 130$ GeV, the width is quite large, $\Gamma_2 = 263$ GeV($\theta = 0$) and $\Gamma_2 = 295$ GeV($\theta = \pi/12$)³. We have included the width using the Breit-Wigner approximation, although typically $\Gamma_2/m_2 \sim \mathcal{O}(\frac{1}{2})$. The shoulder due to the width is clear on the LHS of Fig. 4. There is a smaller width for h_2 when m_3 is increased to 250 GeV: $\Gamma_2 = 129$ GeV($\theta = 0$) and $\Gamma_2 = 137$ GeV($\theta = \pi/12$) on the RHS of Fig. 4. The widths are calculated by scaling the SM results from Ref. [36] with the appropriate mixing angles and adding the relevant widths $h_i \rightarrow h_j h_k$.

In Figs. 6 and 7, we show mass regions where the rate for $h_1 h_3$ production is significantly enhanced relative to the SM $h_1 h_1$ production. This enhancement can be traced to the

¹ For the complex singlet model with a $U(1)$ symmetry, a comparable scan can be performed using the program ScannerS[19].

² $M_{hh} \equiv (p_{h_1} + p_{h_3})^2$.

³ The parameters of the $\theta_2 = 0$ curve on the LHS of Fig. 4 are, for example, $\delta_2 = 21.6$, $Re(\delta_3) = -14.5$, $Im(\delta_3) = -22.9$, $Re(d_1) = 1.15$, $Im(d_1) = 1.64$, $d_2 = 13.3$, $Re(d_3) = 10.5$, $Im(d_3) = 10.2$, $Re(e_1) = 1.18v$, $Im(e_1) = -2.66v$, $Re(e_2) = -8.29v$, $Im(e_2) = 3.67v$. These parameters correspond to $\lambda_{211} = -2.9v$, $\lambda_{311} = 6.77v$, $\lambda_{321} = -11.1v$ and $\lambda_{331} = 11.2v$.

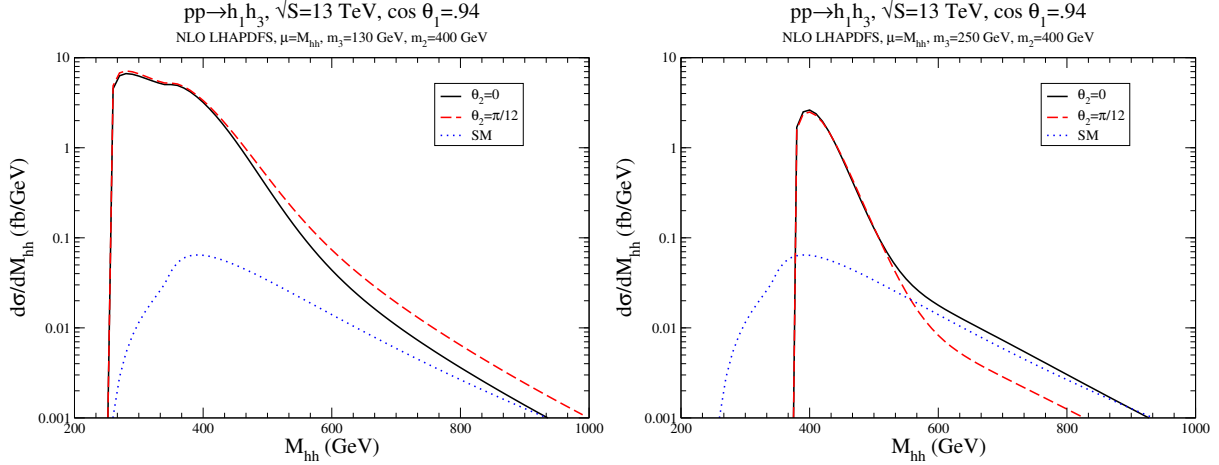


FIG. 5: M_{hh} spectrum of the complex singlet model production of $h_1 h_3$ from the resonant exchange of h_2 . The dominant contribution in the loops is from the top quark.

relatively large values of the tri-linear Higgs couplings defined from Eq. 1,

$$\mathcal{V} \rightarrow \frac{1}{2} \lambda_{211} h_1^2 h_2 + \frac{1}{2} \lambda_{311} h_1^2 h_3 + \frac{1}{2} \lambda_{331} h_1 h_3^2 + \lambda_{321} h_1 h_2 h_3 + \dots, \quad (17)$$

that are allowed by the imposed restrictions. In the SM, the hhh coupling is fixed by m_h , whereas here, the trilinear couplings of the potential are relatively unconstrained. In Fig. 8, we show the region of parameter space allowed by limits on the oblique parameters, perturbative unitarity, and the minimization of the potential where the $h_1 h_1 h_1$ tri-linear coupling is greater than 5 times the SM value. This enhancement of the tri-linear scalar coupling requires rather light values of m_2 and m_3 as shown in Fig. 8. In roughly the same region as shaded in Fig. 8, the $h_2 h_1 h_1$ and $h_3 h_2 h_1$ couplings are 8 times the SM $h_1 h_1 h_1$ coupling. This enhancement is consistent with the results of Ref. [21] in the complex singlet model with a global $U(1)$ symmetry imposed on the potential. The cut-offs on the high m_2 ends of the plots on the LHS in Figs. 6 and 7 are due to the oblique parameter restrictions in the non-zero θ_2 mixing scenario. The same results for $\sqrt{S} = 27$ and 100 TeV are shown in Fig. 7. At all energies there is a significant region of phase space where the $h_1 h_3$ rate is large, relative to SM double Higgs production.

For $m_3 > 250$ GeV, the dominant decay chain from $h_1 h_3$ production will be $h_1 h_3 \rightarrow h_1 h_1 h_1 \rightarrow (b\bar{b})(b\bar{b})(b\bar{b})$. For $m_3 < 2m_1$, h_3 will decay through the extremely small couplings to SM particles and through the off-shell decay $h_3 \rightarrow h_1 h_1^* \rightarrow h_1 f \bar{f}$ and will be extremely long lived. In the limiting case where $\theta_2 = 0$, the only allowed decay for h_3 is the off-shell

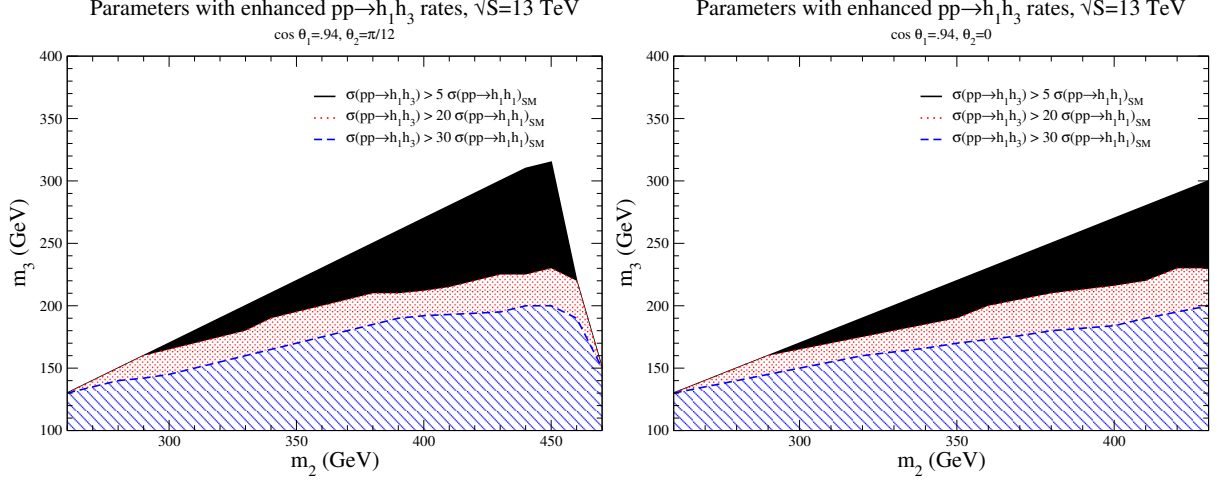


FIG. 6: Regions of parameter space allowed by limits on oblique parameters, perturbative unitarity, and the minimization of the potential where the rate for $h_1 h_3$ production is significantly larger than the SM $h_1 h_1$ rate at $\sqrt{S} = 13 \text{ TeV}$.

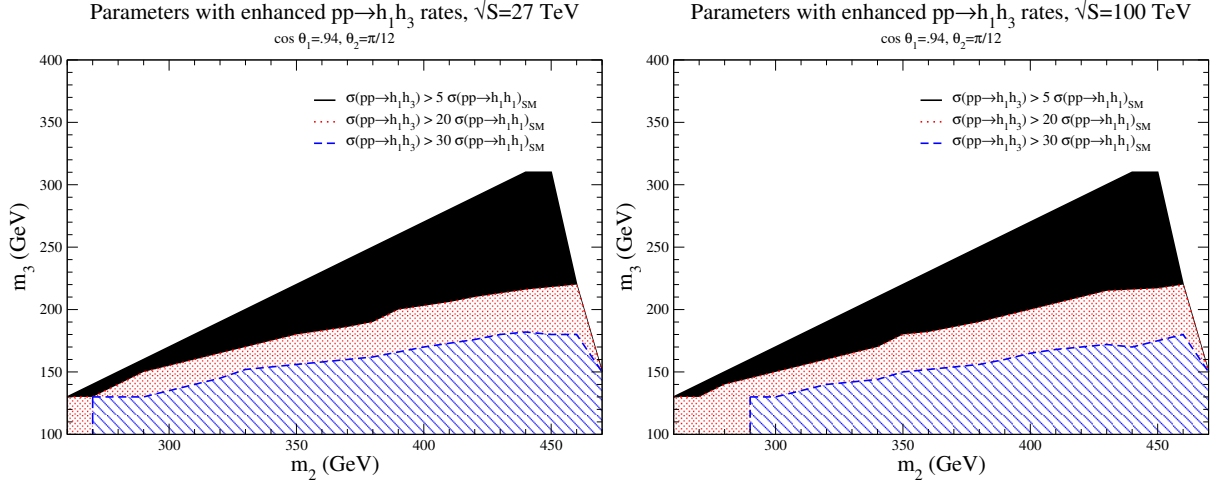


FIG. 7: Regions of parameter space allowed by limits on oblique parameters, perturbative unitarity, and the minimization of the potential where the rate for $h_1 h_3$ production is significantly larger than the SM $h_1 h_1$ rate at $\sqrt{S} = 27 \text{ TeV}$ and 100 TeV .

decay chain through the couplings to h_1 .

V. CONCLUSIONS

We have studied an extension of the SM with a complex scalar singlet. We considered the most general renormalizable scalar potential and imposed no additional symmetries. In

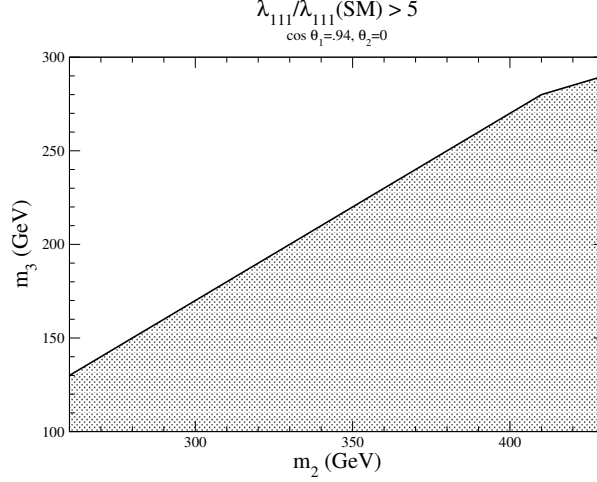


FIG. 8: Region of parameter space allowed by limits on oblique parameters, perturbative unitarity, and the minimization of the potential where the $h_1 h_1 h_1$ tri-linear coupling is greater than 5 times the SM value.

this scenario, there are 3 scalar bosons, one of which, h_3 , has very small couplings to SM particles and will be primarily observed through di-Higgs decays, $h_2 \rightarrow h_1 h_3$. Subject to the constraints of electroweak precision measurements, single Higgs production rates, and perturbative unitarity, there are regions of phase space where the rate for $h_1 h_3$ production is significantly enhanced relative to the SM $h_1 h_1$ rate. Therefore, the search for pair production of Higgs bosons with different masses is a distinctive signature of this class of model.

Acknowledgements

S.D. is supported by the U.S. Department of Energy under grant No. DE-AC02-98CH10886 and contract DE-AC02-76SF00515. M.S. is supported by the U.S. Department of Energy, Office of Science, Office of Workforce Development for Teachers and Scientists, Office of Science Graduate Student Research (SCGSR) program. The SCGSR program is administered by the Oak Ridge Institute for Science and Education (ORISE) for the DOE. ORISE is managed by ORAU under contract number DE-SC0014664. We thank I.M. Lewis for discussions.

[1] T. Plehn, M. Spira, and P. Zerwas, Nucl.Phys. **B479**, 46 (1996), hep-ph/9603205.

- [2] R. Frederix *et al.*, Phys. Lett. **B732**, 142 (2014), 1401.7340.
- [3] ATLAS Collaboration, CERN Report No. ATLAS-CONF-2016-049, 2016 (unpublished).
- [4] U. Baur, T. Plehn, and D. L. Rainwater, Phys.Rev. **D67**, 033003 (2003), hep-ph/0211224.
- [5] M. J. Dolan, C. Englert, and M. Spannowsky, JHEP **1210**, 112 (2012), 1206.5001.
- [6] J. Baglio *et al.*, JHEP **1304**, 151 (2013), 1212.5581.
- [7] V. Barger, L. L. Everett, C. Jackson, A. Peterson, and G. Shaughnessy, (2014), 1408.0003.
- [8] V. Barger, P. Langacker, M. McCaskey, M. J. Ramsey-Musolf, and G. Shaughnessy, Phys.Rev. **D77**, 035005 (2008), 0706.4311.
- [9] S. Profumo, M. J. Ramsey-Musolf, and G. Shaughnessy, JHEP **0708**, 010 (2007), 0705.2425.
- [10] G. M. Pruna and T. Robens, Phys.Rev. **D88**, 115012 (2013), 1303.1150.
- [11] C.-Y. Chen, S. Dawson, and I. M. Lewis, Phys. Rev. **D91**, 035015 (2015), 1410.5488.
- [12] S. Dawson and I. M. Lewis, Phys. Rev. **D92**, 094023 (2015), 1508.05397.
- [13] I. M. Lewis and M. Sullivan, Phys. Rev. **D96**, 035037 (2017), 1701.08774.
- [14] J. M. No and M. Ramsey-Musolf, Phys. Rev. **D89**, 095031 (2014), 1310.6035.
- [15] J. R. Espinosa, T. Konstandin, and F. Riva, Nucl.Phys. **B854**, 592 (2012), 1107.5441.
- [16] S. Profumo, M. J. Ramsey-Musolf, C. L. Wainwright, and P. Winslow, (2014), 1407.5342.
- [17] D. Curtin, P. Meade, and C.-T. Yu, (2014), 1409.0005.
- [18] C.-Y. Chen, J. Kozaczuk, and I. M. Lewis, JHEP **08**, 096 (2017), 1704.05844.
- [19] R. Coimbra, M. O. P. Sampaio, and R. Santos, Eur. Phys. J. **C73**, 2428 (2013), 1301.2599.
- [20] M. Gonderinger, H. Lim, and M. J. Ramsey-Musolf, Phys. Rev. **D86**, 043511 (2012), 1202.1316.
- [21] R. Costa, M. Muhlleitner, M. O. P. Sampaio, and R. Santos, JHEP **06**, 034 (2016), 1512.05355.
- [22] M. Muhlleitner, M. O. P. Sampaio, R. Santos, and J. Wittbrodt, JHEP **08**, 132 (2017), 1703.07750.
- [23] V. Barger, P. Langacker, M. McCaskey, M. Ramsey-Musolf, and G. Shaughnessy, Phys. Rev. **D79**, 015018 (2009), 0811.0393.
- [24] ATLAS, G. Aad *et al.*, JHEP **11**, 206 (2015), 1509.00672.
- [25] ATLAS, CMS, G. Aad *et al.*, JHEP **08**, 045 (2016), 1606.02266.
- [26] S. Dawson and W. Yan, Phys. Rev. **D79**, 095002 (2009), 0904.2005.
- [27] J. de Blas *et al.*, JHEP **12**, 135 (2016), 1608.01509.
- [28] ATLAS, M. Aaboud *et al.*, (2017), 1710.01123.

- [29] CMS, V. Khachatryan *et al.*, JHEP **10**, 144 (2015), 1504.00936.
- [30] D. Lopez-Val and T. Robens, Phys. Rev. **D90**, 114018 (2014), 1406.1043.
- [31] G. Chalons, D. Lopez-Val, T. Robens, and T. Stefaniak, PoS **DIS2016**, 113 (2016), 1606.07793.
- [32] B. W. Lee, C. Quigg, and H. B. Thacker, Phys. Rev. **D16**, 1519 (1977).
- [33] M. Bowen, Y. Cui, and J. D. Wells, JHEP **0703**, 036 (2007), hep-ph/0701035.
- [34] J. Butterworth *et al.*, J. Phys. **G43**, 023001 (2016), 1510.03865.
- [35] A. Buckley *et al.*, Eur. Phys. J. **C75**, 132 (2015), 1412.7420.
- [36] LHC Higgs Cross Section Working Group, S. Dittmaier *et al.*, (2011), 1101.0593.